ELSEVIER

Journal of Organometallic Chemistry 658 (2002) 117–125

Journal of Organometallic Chemistry

www.elsevier.com/locate/jorganchem

Syntheses and structures of some coordinatively saturated and unsaturated diruthenium carbonyl complexes

Kom-Bei Shiu [a,*], Jiun-Yu Chen [a], Gene-Hsiang Lee [b], Fen-Ling Liao [c], Bao-Tsan Ko [d], Yu Wang [b], Sue-Lein Wang [c], Chu-Chieh Lin [d]

[a] *Department of Chemistry, National Cheng Kung University, 701 Tainan, Taiwan, ROC*
[b] *Instrument Center, National Taiwan University, 107 Taipei, Taiwan, ROC*
[c] *Instrument Center, National Tsing-Hua University, 300 Hsinchu, Taiwan, ROC*
[d] *Instrument Center, National Chung-Hsing University, 402 Taichung, Taiwan, ROC*

Received 13 April 2002; received in revised form 13 May 2002; accepted 27 May 2002

Abstract

Reaction of $[Ru_2(CO)_4(\mu\text{-DPPM})_2(\mu\text{-OAc})][PF_6]$ (**1**) with $Et_3O^+BF_4^-$ in MeCN produced coordinatively saturated $[Ru_2(\mu\text{-CO})_2(\mu\text{-DPPM})_2(MeCN)_4][BF_4]_2$ (**2**). Upon addition of an excess amount of a uni-negative anion X^- to a solution of **2** in MeCN, a series of neutral, coordinatively unsaturated adducts $[Ru_2(\mu\text{-CO})_2(\mu\text{-DPPM})_2X_2]$ ($X^- = Cl^-$, **3a**; Br^-, **3b**; I^-, **3c**; SH^-, **3d**; $Stol^-$, **3e**; S^iPr^-, **3f**) were readily formed. The reaction of **3a** with trimethylamine *N*-oxide dihydrate produced two isomeric products of $[Ru_2(CO)_2(\mu\text{-DPPM})_2Cl_2(\mu\text{-H})(\mu\text{-OH})]$ at a ratio of **4a**–**4b** = 2.25. Treatment of **3b** and **3c** with dimethyl acetylenedicarboxylate produced $[Ru_2(\mu\text{-CO})(\mu\text{-DPPM})_2(\mu\text{-MeO}_2CCCCO_2Me)X_2]$ (X = Br, **5a**; I, **5b**), whereas treating of **3e** and **3f** with I_2 yielded $[Ru_2(CO)_2(\mu\text{-DPPM})_2I_2(\mu\text{-I})(\mu\text{-SR})]$ (R = tol, **6a**; ^{i}Pr, **6b**). The structures of **2**, **3a**, **3c**, **3e**, **4b**, **5a** and **6a** were determined by X-ray crystallography. The observed Ru–Ru distances are compared and explained in terms of both electronic and steric effects by considering the multiple metal–ligand (M–X) bonding interactions and Alvarez's structural parameters including M–M–X pyramidal angles and the X–M–M–X torsional angles.

Keywords: Ruthenium; Carbonyl; Coordinatively unsaturated adducts

1. Introduction

In a previous communication [1], we reported briefly unusual transformations from $[Ru_2(CO)_4(\mu\text{-DPPM})_2(\mu\text{-OAc})][PF_6]$ (**1**) to $[Ru_2(\mu\text{-CO})_2(\mu\text{-DPPM})_2(MeCN)_4][BF_4]_2$ (**2**), from **2** to $[Ru_2(\mu\text{-CO})_2(\mu\text{-DPPM})_2X_2]$ ($X^- = Cl^-$, **3a**; Br^-, **3b**; I^-, **3c**; SH^-, **3d**; $Stol^-$, **3e**; S^iPr^-, **3f**) and from **3a** to $[Ru_2(CO)_2(\mu\text{-DPPM})_2Cl_2(\mu\text{-H})(\mu\text{-OH})]$ in two isomers of **4a** and **4b**. Compounds **3a**–**f** appear to contain a formal Ru–Ru triple bond, based on the 18-electron rule, but this assignment is not supported by the observed Ru–Ru distance of **3c**. In this contribution, we wish to describe all these transformations in detail plus two solid-state structures for **3a** and **3e**, and two new reactions for **3b**, **3c**, **3e**, and **3f** (Schemes 1–3, vide infra). The Ru–Ru distances found will be compared and explained in terms of both electronic and steric effects by considering the multiple metal–ligand (M–X) bonding interactions [2] and Alvarez's structural parameters including M–M–X pyramidal angles and the X–M–M–X torsional angles [3].

2. Experimental

All solvents were dried and purified by standard methods and were freshly distilled under nitrogen immediately before use. All reactions and manipulations were carried out in standard Schlenk ware, connected to a switchable double manifold providing vacuum and nitrogen. Reagents were used as supplied by Aldrich, Fluka, or Strem. ^{1}H- and ^{31}P-NMR spectra were measured on a Brueker AMC-400 (^{1}H, 400 MHz; ^{31}P-

* Corresponding author. Fax: +886-6-274-0552
E-mail address: kbshiu@mail.ncku.edu.tw (K.-B. Shiu).

0022-328X/02/$ - see front matter
PII: S0022-328X(02)01636-4

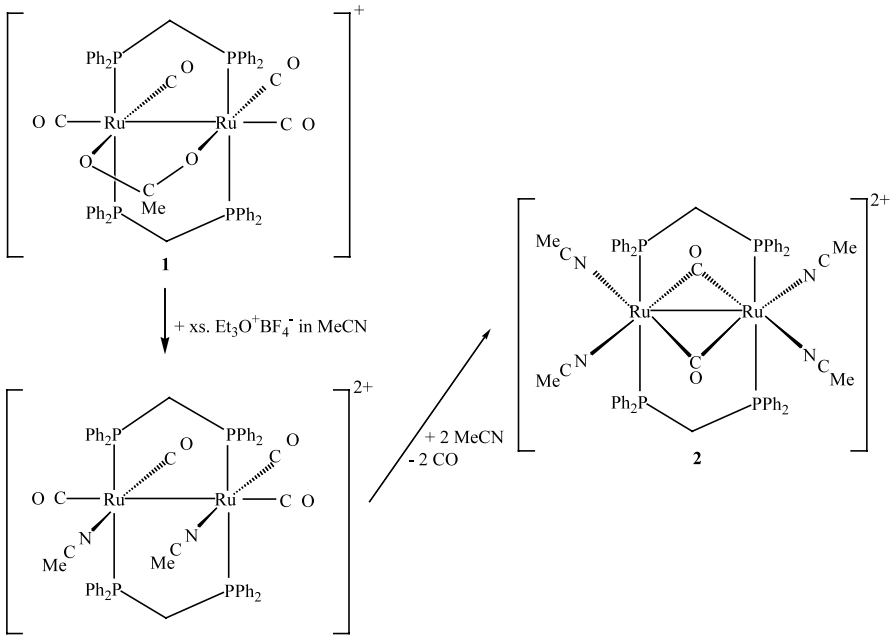

Scheme 1.

NMR, 162 MHz) NMR spectrometer. ^{1}H chemical shifts (δ in ppm, J in Hz) are defined as positive downfield relative to internal Me_4Si (TMS) or the deuterated solvent, while ^{31}P chemical shifts are referred to external 85% H_3PO_4. The IR spectra were recorded on a BioRad FTS 175 instrument. Microanalyses were carried out by the staff of the Microanalytical Service of the Department of Chemistry, National Cheng Kung University.

2.1. Synthesis of $[Ru_2(\mu\text{-}CO)_2(\mu\text{-}DPPM)_2(MeCN)_4][BF_4]_2$ (2)

In a 100 ml Schlenk flask was added $[Ru_2(CO)_4(\mu\text{-}DPPM)_2(\mu\text{-}OAc)][BF_4]$ (**1**) [4] (1.753 g, 1.426 mmol), 20 ml of MeCN, and 4 ml of 1 M $Et_3O^+BF_4^-$ solution in CH_2Cl_2 at ambient temperature. The mixture was then heated at 82 °C for 17 h and cooled to ambient temperature. The volume of the solution was reduced

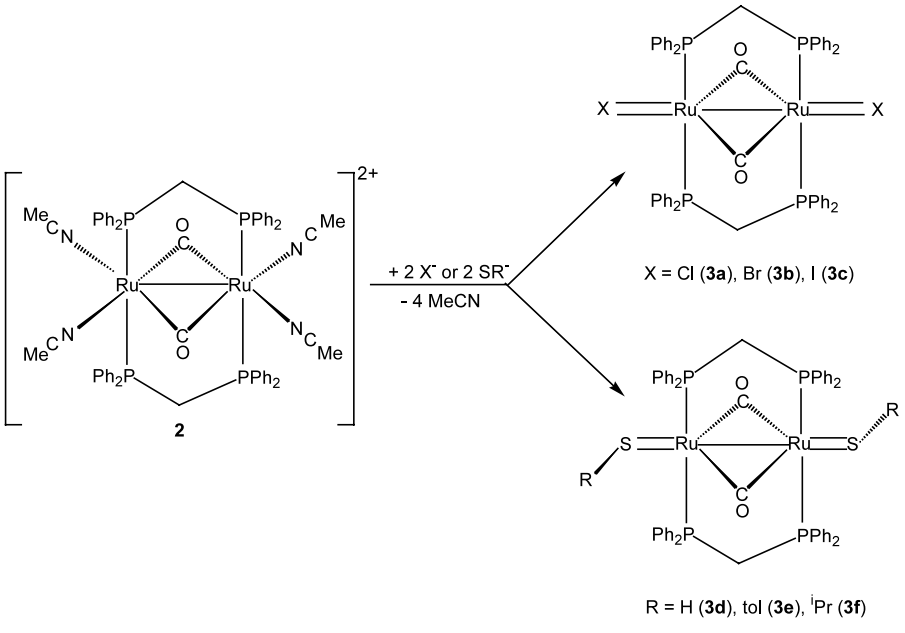

Scheme 2.

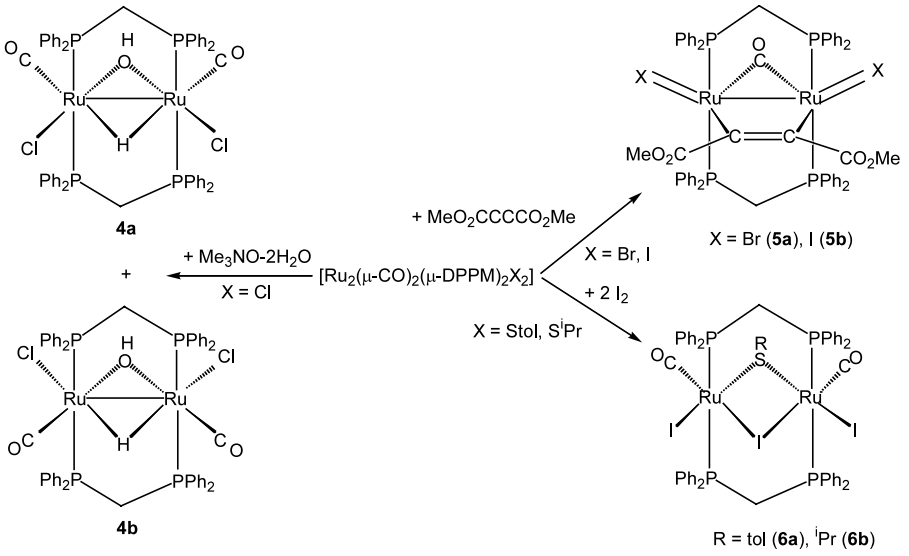

Scheme 3.

to ca. 0.5 and 10 ml of MeOH was then added. Filtration gave a pink solid **2**, which was washed with 5 ml of MeOH and dried under vacuum. Yield 1.557 g (80%). Compound **2**: Anal. Calc. for $C_{60}H_{56}B_2F_8N_4O_2P_4Ru_2$: C, 52.80; H, 4.14; N, 4.11. Found: C, 52.77; H, 4.13; N, 4.08%. ^{1}H-NMR (CD_3CN, 400 MHz): δ 1.97 (s, CH_3CN, 12 H), 3.03 (quin, $J_{P,\ H} = 4.8$, $Ph_2PCH_2PPh_2$, 4 H), 7.28 (m, *Ph*, 24 H), 7.46 (m, *Ph*, 16 H). ^{13}C{^{1}H}-NMR (acetone-d_6, 100 MHz): δ 0.83 (quin, $J_{P,\ C} = 21$, CH_3CN, 4 C), 19.65 (quin, $J_{P,\ C} = 11$, $Ph_2PCH_2PPh_2$, 2 C), 119.06 (br, CH_3CN, 4 C), 258.53 (s, *C*O, 2 C), and the phenyl carbon atoms at 129.62 (br, 16 C), 131.42 (quin, $J_{P,\ C} = 12.5$, 8 C), 131.93 (br, 8 C), 133.74 (br, 16 C). ^{31}P{^{1}H}-NMR (CD_3CN, 162 MHz): δ 28.52 (s, 4 P). IR (Nujol): ν(CN), 2317w, 2309w, 2286w, 2280w; ν(CO), 1683s, 1661sh cm^{-1}. IR: ν(CO), 1736s cm^{-1} in CH_2Cl_2 and 1700 cm^{-1} in CH_3CN.

2.2. Synthesis of $[Ru_2(\mu\text{-}CO)_2(\mu\text{-}DPPM)_2X_2]$ ($X^- = Cl^-$, **3a**; Br^-, **3b**; I^-, **3c**; SH^-, **3d**; $Stol^-$, **3e**; S^iPr^-, **3f**)

The preparation procedures for **3a**–**f** are all similar, and a typical procedure for **3c** is described below. In a 100 ml Schlenk flask was added **2** (0.100 g, 0.073 mmol), NaI (0.055 g, 0.367 mmol), and 10 ml of MeCN at ambient temperature. The mixture was then stirred for 1 h. Filtration gave the orange–yellow product, which was then recrystallized from CH_2Cl_2–MeCN and dried in vacuo to give 0.062 g (67%). Compound **3a**: Anal. Calc. for $C_{52}H_{44}Cl_2O_2P_4Ru_2$: C, 56.89; H, 4.04. Found: C, 56.73; H, 4.15%. ^{1}H-NMR (acetone-d_6, 400 MHz): δ 2.59 (br, $Ph_2PCH_2PPh_2$, 4 H), 7.28 (m, *Ph*, 24 H), 7.60 (m, *Ph*, 16 H). ^{31}P{^{1}H}-NMR (CD_2Cl_2, 162 MHz): δ 28.66 (s, 4 P). IR (CH_2Cl_2): ν(CO), 1750w, 1702s cm^{-1}. Compound **3b**: Anal. Calc. for $C_{52}H_{44}Br_2O_2P_4Ru_2$: C, 53.10; H, 3.70. Found: C, 53.02; H, 3.64%. ^{1}H-NMR (acetone-d_6, 400 MHz): δ 2.97 (quin, $J_{P,\ H} = 4.4$, $Ph_2PCH_2PPh_2$, 4 H), 7.28 (m, *Ph*, 24 H), 7.69 (m, *Ph*, 16 H). ^{31}P{^{1}H}-NMR (acetone-d_6, 162 MHz): δ 32.30 (s, 4 P). IR (CH_2Cl_2): ν(CO), 1750w, 1702s cm^{-1}. Compound **3c**: Anal. Calc. for $C_{52}H_{44}I_2O_2P_4Ru_2$: C, 48.77; H, 3.46. Found: C, 48.64; H, 3.45%. ^{1}H-NMR (acetone-d_6, 400 MHz): δ 3.07 (quin, $J_{P,\ H} = 4.4$, $Ph_2PCH_2PPh_2$, 4 H), 7.26 (m, *Ph*, 24 H), 7.71 (m, *Ph*, 16 H). ^{31}P{^{1}H}-NMR (acetone-d_6, 162 MHz): δ 29.06 (s, 4 P). IR (CH_2Cl_2): ν(CO), 1747w, 1702s cm^{-1}. Compound **3d**: Anal. Calc. for $C_{52}H_{46}O_2P_4Ru_2S_2$: C, 57.14; H, 4.24. Found: C, 57.08; H, 4.17%. ^{1}H-NMR (acetone-d_6, 400 MHz): δ 2.98 (quin, $J_{P,\ H} = 4.6$, $Ph_2PCH_2PPh_2$, 4 H), 7.30 (m, *Ph*, 24 H), 7.70 (m, *Ph*, 16 H). ^{31}P{^{1}H}-NMR (acetone-d_6, 162 MHz): δ 33.93 (s, 4 P). IR (CH_2Cl_2): ν(CO), 1704s cm^{-1}. Compound **3e**: Anal. Calc. for $C_{66}H_{58}O_2P_4Ru_2S_2$: C, 62.26; H, 4.59. Found: C, 62.21; H, 4.56%. ^{1}H-NMR (CD_2Cl_2, 400 MHz): δ 1.90 (s, $SC_6H_4CH_3$, 6 H), 2.73 (quin, $J_{P,\ H} =$ 4.4, $Ph_2PCH_2PPh_2$, 4 H), 5.96 (d, $J_{H,\ H} = 7.9$, 4 H) and 6.04 (d, $J_{H,\ H} = 7.9$, 4 H) for $SC_6H_4CH_3$, 7.49 (m, *Ph*, 24 H), 7.85 (m, *Ph*, 16 H). ^{31}P{^{1}H}-NMR (CD_2Cl_2, 162 MHz): δ 33.86 (s, 4 P). IR (CH_2Cl_2): ν(CO), 1688s cm^{-1}. Compound **3f**: Anal. Calc. for $C_{58}H_{58}O_2P_4Ru_2S_2CH_2Cl_2$: C, 56.12; H, 4.79. Found: C, 55.91; H, 4.76%. ^{1}H-NMR (acetone-d_6, 400 MHz): δ 0.24 (d, $J_{H,\ H} = 6.6$, $CH(CH_3)_2$, 12 H), 2.62 (hept, $J_{H,\ H} = 6.6$, $CH(CH_3)_2$, 2 H), 2.70 (quin, $J_{P,\ H} = 4.4$, $Ph_2PCH_2PPh_2$, 4 H), 7.25 (m, *Ph*, 24 H), 7.79 (m, *Ph*, 16 H). ^{31}P{^{1}H}-NMR (CD_2Cl_2, 162 MHz): δ 30.57 (s, 4 P). IR (CH_2Cl_2): ν(CO), 1682s cm^{-1}.

2.3. Reaction between $[Ru_2(\mu\text{-}CO)_2(\mu\text{-}DPPM)_2Cl_2]$ (**3a**) and trimethylamine N-oxide dihydrate

The solution of **3a** (0.158 g, 0.144 mmol) in 10 ml of CH_2Cl_2 was added dropwise with 2.1 ml of the Me_3NO solution, prepared from $Me_3NO{\cdot}2H_2O$ (0.100 g, 0.901 mmol) dissolved in 10 ml of MeOH. The solution was stirred for 36 h and the volatiles were pumped off. Two isomeric products of $[Ru_2(CO)_2(\mu\text{-}DPPM)_2Cl_2(\mu\text{-}H)(\mu\text{-}OH)]$ were separated as a major and a minor yellow bands, respectively, by thin-layer chromatography (TLC) (silica gel, CH_2Cl_2–hexane = 6:1) in a glove box, using TLC plates (Kieselguhr 60 F254, E. Merk), and recrystallized from CH_2Cl_2–hexane, producing 25 mg (16% yield) of **4a** and 8 mg (5%) of **4b**. Anal. Calc. for $C_{52}H_{44}Cl_2O_3P_4Ru_2{\cdot}2H_2O$: C, 54.32; H, 4.21. Found: C, 54.36; H, 4.19%. For **4a**: ^{1}H-NMR (CD_2Cl_2, 400 MHz): δ −26.36 (quin, $J_{P,\,H} = 8.4$, μ-H, 1 H), 2.12 (br, μ-OH, 1 H), 3.18 (m, $Ph_2PCH_2PPh_2$, 2 H), 3.97 (m, $Ph_2PCH_2PPh_2$, 2 H), 7.20 (m, *Ph*, 40 H). $^{31}P\{^1H\}$-NMR (CD_2Cl_2, 162 MHz): δ 6.16 (s, 4 P). IR (CH_2Cl_2): ν(OH), 3627w; ν(CO), 1978s, 1964sh cm^{-1}. For **4b**: ^{1}H-NMR (CD_2Cl_2, 400 MHz): δ −25.06 (quin, $J_{P,\,H} = 8.4$, μ-H, 1 H), 2.12 (br, μ-OH, 1 H), 3.12 (m, $Ph_2PCH_2PPh_2$, 2 H), 3.67 (m, $Ph_2PCH_2PPh_2$, 2 H), 7.32 (m, *Ph*, 40 H). $^{31}P\{^1H\}$-NMR (CD_2Cl_2, 162 MHz): δ 8.76 (s, 4 P). IR (CH_2Cl_2): ν(OH), 3615w; ν(CO), 1968s, 1954sh cm^{-1}.

2.4. Reaction between $[Ru_2(\mu\text{-}CO)_2(\mu\text{-}DPPM)_2X_2]$ (X = Br, **3b**; X = I, **3c**) and dimethyl acetylenedicarboxylate

The suspension of **3b** (0.116 g, 0.098 mmol) and 0. 5 ml of dimethyl acetylenedicarboxylate (ca. 4.07 mmol) in 18 ml of THF were heated under reflux for 16.5 h and the volatiles were pumped off. Recrystallization from CH_2Cl_2–MeOH gave 77 mg (60% yield) of $[Ru_2(\mu\text{-}CO)(\mu\text{-}DPPM)_2(\mu\text{-}MeO_2CCCCO_2Me)Br_2]$ (**5a**). Compound $[Ru_2(\mu\text{-}CO)(\mu\text{-}DPPM)_2(\mu\text{-}MeO_2CCCCO_2Me)I_2]$ (**5b**) were prepared similarly from **3c**. Yield 69%. Compound **5a**: Anal. Calc. for $C_{57}H_{50}Br_2O_5P_4Ru_2$: C, 52.63; H, 3.87. Found: C, 52.37; H, 4.18%. ^{1}H-NMR (CD_2Cl_2, 400 MHz): δ 2.08 (s, COO*Me*, 6 H), 2.19 (m, $Ph_2PCH_2PPh_2$, 2 H), 3.16 (m, $Ph_2PCH_2PPh_2$, 2 H), 7.33 (m, *Ph*, 40 H). $^{31}P\{^1H\}$-NMR (CD_2Cl_2, 162 MHz): δ 12.88 (s, 4 P). IR (CH_2Cl_2): ν(CO), 1731s (COOMe), 1704s (μ-CO) cm^{-1}. Compound **5b**: Anal. Calc. for $C_{57}H_{50}I_2O_5P_4Ru_2$: C, 49.08; H, 3.61. Found: C, 48.85; H, 3.39%. ^{1}H-NMR (CD_2Cl_2, 400 MHz): δ 2.08 (s, COO*Me*, 6 H), 2.36 (m, $Ph_2PCH_2PPh_2$, 2 H), 3.41 (m, $Ph_2PCH_2PPh_2$, 2 H), 7.25 (m, *Ph*, 40 H). $^{31}P\{^1H\}$-NMR (CD_2Cl_2, 162 MHz): δ 14.33 (s, 4 P). IR (CH_2Cl_2): ν(CO), 1729s (COOMe), 1702s (μ-CO) cm^{-1}.

2.5. Reaction between $[Ru_2(\mu\text{-}CO)_2(\mu\text{-}DPPM)_2X_2]$ (X = Stol, **3e**; S^iPr, **3f**) and I_2

The solution of **3e** (0.512 g, 0.402 mmol) in 10 ml of CH_2Cl_2 was added dropwise with 7.8 ml of an I_2 solution prepared by dissolving 0.210 g of I_2 (0.0827 mmol) in 10 ml of CH_2Cl_2. The solution was stirred for 1 h and the volatiles were pumped off. One major orange–red band was separated by TLC (silica gel, CH_2Cl_2–hexane = 1:1) in a glove box, using TLC plates (Kieselguhr 60 F254, E. Merk), and recrystallized from CH_2Cl_2–MeOH, producing 0.258 g (41% yield) of $[Ru_2(CO)_2(\mu\text{-}DPPM)_2I_2(\mu\text{-}I)(\mu\text{-}Stol)]$ (**6a**). Compound $[Ru_2(CO)_2(\mu\text{-}DPPM)_2I_2(\mu\text{-}I)(\mu\text{-}S^iPr)]$ (**6b**) was prepared similarly from **3f**. Yield 21%. Compound **6a**: Anal. Calc. for $C_{61}H_{51}I_3O_2P_4Ru_2S$: C, 47.12; H, 3.31. Found: C, 47.05; H, 3.32%. ^{1}H-NMR (CD_2Cl_2, 400 MHz): δ 2.38 (s, $C_6H_4CH_3$, 3 H), 4.04 (m, $Ph_2PCH_2PPh_2$, 2 H), 4.36 (m, $Ph_2PCH_2PPh_2$, 2 H), 6.56 (d, $J_{H,\,H} = 7.9$, $C_6H_4CH_3$, 2 H), 6.85 (d, $J_{H,\,H} = 7.9$, $C_6H_4CH_3$, 2 H), 7.20 (m, *Ph*, 40 H). $^{31}P\{^1H\}$-NMR (CD_2Cl_2, 162 MHz): δ 3.66 (s, 4 P). IR (CH_2Cl_2): ν(CO), 1968s cm^{-1}. Compound **6b**: Anal. Calc. for $C_{55}H_{51}I_3O_2P_4Ru_2S{\cdot}CH_2Cl_2$: C, 42.90; H, 3.41. Found: C, 42.60; H, 3.36%. ^{1}H-NMR (CD_2Cl_2, 400 MHz): δ 0.69 (d, $J_{H,\,H} = 6.6$, $CH(CH_3)_2$, 3 H), 2.74 (hept, $J_{H,\,H} = 6.6$, $CH(CH_3)_2$, 1 H), 4.02 (m, $Ph_2PCH_2PPh_2$, 2 H), 4.41 (m, $Ph_2PCH_2PPh_2$, 2 H), 7.24 (m, *Ph*, 24 H), 7.80 (m, *Ph*, 16 H). $^{31}P\{^1H\}$-NMR (CD_2Cl_2, 162 MHz): δ 2.89 (s, 4 P). IR (CH_2Cl_2): ν(CO), 1968s cm^{-1}.

2.6. X-ray data collection, solution, and refinement

Suitable single crystals of **2**, **3a**, **3c**, **3e**, **4b**, **5a** and **6a** were grown from CH_2Cl_2–MeOH or CH_2Cl_2–hexane at room temperature and chosen for single crystal structure determinations. All the X-ray diffraction data were measured in frames with increasing ω (width of 0.3° per frame) and with the scan speed at 20.00 s per frame on a Siemens SMART-CCD instrument, equipped with a normal focus and 3 kW sealed-tube X-ray source. Empirical absorption corrections were carried out using SHELXTL-PC program for **2** and **4b**, and SADABS program for **3a**, **3c**, **3e**, **5a** and **6a**. The latter four structures were solved by the heavy-atom method and refined by a full-matrix least-squares procedure using NRCVAX [5]. Structures **2**, **3a** and **5b** were solved by direct methods and refined by a full-matrix least-squares procedure using SHELXTL-PLUS [6]. Neutral atom scattering factors for non-hydrogen atoms and the values for $\Delta f'$ and $\Delta f''$ described in each software were used [5,6]. The other essential details of single-crystal data measurement and refinement are listed in Table 1. In structure **3e**, two atomic positions with 0.5 occupancy were found for atoms C(20) and C(21) of one phenyl group attached to P(2).

Table 1
Crystal data

	2	**3a**	**3c**·$2CH_2Cl_2$	**3e**	**4b**·$2H_2O$	**5a**·$2CH_2Cl_2$	**6a**·CH_3CN
Empirical formula	$C_{30}H_{28}BF_4N_2O$-P_2Ru	$C_{26}H_{22}ClO_2$-P_2Ru	$C_{54}H_{48}Cl_4I_2O_2$-P_4Ru_2	$C_{66}H_{58}O_2$-$P_4Ru_2S_2$	$C_{52}H_{50}Cl_2O_5$-P_4Ru_2	$C_{59}H_{54}Br_2Cl_4$-$O_5P_4Ru_2$	$C_{61}H_{54}I_3NO_2$-P_4Ru_2S
Formula weight (fw)	682.36	548.90	1450.62	1273.26	1151.84	1470.66	1571.83
Space group	$P2_1/c$	$C2/c$	$Pna2_1$	$P2_1/n$	$Pna2_1$	$P2_1/c$	$Pbca$
a (Å)	11.3231(2)	18.4917(10)	29.302(5)	11.4620(3)	24.0411(9)	12.7529(3)	18.637(4)
b (Å)	17.6611(1)	13.4267(7)	15.541(2)	13.0843(3)	12.4778(5)	15.8030(3)	21.572(2)
c (Å)	16.0614(2)	20.7276(12)	12.329(2)	19.8845(4)	17.6573(7)	28.8517(7)	30.292(4)
α (°)	90	90	90	90	90	90	90
β (°)	110.60(1)	111.439(1)	90	97.503(1)	90	97.951(1)	90
γ (°)	90	90	90	90	90	90	90
V (Å^3)	3006.5(7)	4790.2(5)	5614(2)	2956.6(1)	5296.8(4)	5751.5(2)	12178(3)
Z	4	8	4	2	4	4	8
ρ_{calc} (g cm^{-3})	1.508	1.522	1.716	1.430	1.444	1.698	1.715
μ (mm^{-1})	0.679	0.916	19.591	0.734	0.836	2.261	2.198
λ (Å)	0.71073	0.71073	0.71073	0.71073	0.71073	0.71073	0.71073
Temperature (K)	293(2)	293(2)	298(1)	295(2)	295(2)	120(1)	293(2)
R [a], R_w [b]	0.0556, 0.1431	0.0411, 0.0979	0.049, 0.040	0.0281, 0.0571	0.0442, 0.1155	0.0731, 0.2071	0.0628, 0.936
GOF	1.110	0.719	1.37	1.026	1.006	1.039	1.013

[a] $R = [\Sigma||F_o|-|F_c||/\Sigma|F_o|]$.
[b] $R_w = [\Sigma\ \omega(|F_o|-|F_c|)^2/\Sigma\ \omega|F_o|^2]^{1/2}$.

3. Results and discussion

3.1. Synthesis of $[Ru_2(\mu\text{-}CO)_2(\mu\text{-}DPPM)_2(MeCN)_4]^{2+}$ $[\mathbf{2}]^{2+}$

We previously described that the bridging acetate ligands in $[Ru_2(CO)_4L_2(\mu\text{-}OAc)_2]$ can be removed using alkylating agents such as $Et_3O^+BF_4^-$ in MeCN to form the versatile cations $[Ru_2(CO)_4(MeCN)_4L_2]^{2+}$ [7]. However, when a similar treatment was applied to $[Ru_2(\mu\text{-}CO)_2(\mu\text{-}DPPM)_2(\mu\text{-}OAc)]^+$ $[\mathbf{1}]^+$, both the NMR and IR spectra indicated that the presumed cation $[Ru_2(\mu\text{-}CO)_2(\mu\text{-}DPPM)_2(MeCN)_2]^{2+}$ was indeed formed but then transformed immediately even at the ambient temperature into $[Ru_2(\mu\text{-}CO)_2(\mu\text{-}DPPM)_2(MeCN)_4]^{2+}$ $[\mathbf{2}]^{2+}$ (Scheme 1), isolated as BF_4^- or PF_6^- salts. The structure of $[\mathbf{2}]^{2+}$ (Fig. 1) was confirmed by X-ray diffraction methods to adopt a geometry with idealized D_{2h} symmetry. It contains two bridging carbonyls, two bridging DPPM ligands, and four terminal MeCN ligands. The Ru–Ru distance of 2.7703(7) Å in **2**, a 34-electron complex, is significantly shorter than that of 2.841(1) Å in $[\mathbf{1}]^+$ [4], but still fall in the range of 2.558–3.020 Å observed for typical Ru–Ru single bond distances [4,7,8].

3.2. Reaction of $[Ru_2(\mu\text{-}CO)_2(\mu\text{-}DPPM)_2(CH_3CN)_4]^{2+}$ $[\mathbf{2}]^{2+}$ with uninegative anions

Upon the addition of an excess of the uninegative anion X^- to $[\mathbf{2}]^{2+}$, we obtained, instead of the expected anionic substitution products such as $[Ru_2(\mu\text{-}CO)_2(\mu\text{-}DPPM)_2X_4]^{2-}$, the neutral diamagnetic adducts $[Ru_2(\mu\text{-}CO)_2(\mu\text{-}DPPM)_2X_2]$ ($X^- = Cl^-$, **3a**; Br^-, **3b**; I^-, **3c**; SH^-, **3d**; $Stol^-$, **3e**; S^iPr^-, **3f**) with a formal metal–metal triple bond, assigned for the 30-electron products. Three representative structures, **3a**, **3c** and **3e**, were determined using X-ray diffraction methods. The 'triple' Ru–Ru distances are 2.7430(4) Å in **3a** (Fig. 2), 2.738(2) Å in **3c** (Fig. 3) and 2.8091(3) Å in **3e** (Fig. 4). To our

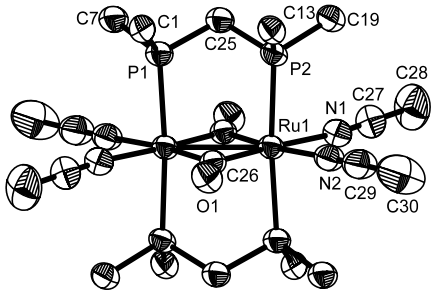

Fig. 1. ORTEP plot of $[\mathbf{2}]^{2+}$ with 50% thermal ellipsoids and the numbering scheme (only the *ipso* carbon atoms of each phenyl group have been retained for clarity). An inversion center is imposed crystallographically at the center of the Ru–Ru bond. Selected bond lengths (Å): Ru(1)–Ru(1′) = 2.7703(7), Ru(1)–P(1) = 2.3875(12), Ru(1)–P(2) = 2.3951(12), Ru(1)–C(26) = 2.002(5), C(26)–O(1) = 1.192(5), Ru(1)–N(1) = 2.156(4), N(1)–C(27) = 1.132(6), C(27)–C(28) = 1.454(8), Ru(1)–N(2) = 2.139(4), N(2)–C(29) = 1.115(6), C(29)–C(30) = 1.465(8). Selected bond angles (°): Ru(1′)–Ru(1)–P(1) = 92.18(3), Ru(1′)–Ru(1)–P(2) = 93.37(3), C(26)–Ru(1)–N(1) = 89.78(17), N(1)–Ru(1)–N(2) = 82.76(16), N(2)–Ru(1)–C(26′) = 93.79(18), C(26′)–Ru(1)–C(26) = 93.71(18), Ru(1)–C(26)–O(1) = 135.3(4), Ru(1)–C(26)–Ru(1′) = 86.29(18), Ru(1)–N(1)–C(27) = 174.4(4), N(1)–C(27)–C(28) = 177.4(6), Ru(1)–N(2)–C(29) = 178.6(5), N(2)–C(29)–C(30) = 177.1(8).

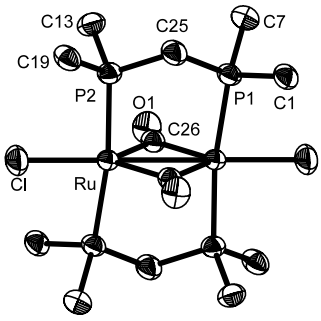

Fig. 2. ORTEP plot of **3a** with 50% thermal ellipsoids and the numbering scheme (only the *ipso* carbon atoms of each phenyl group have been retained for clarity). An inversion center is imposed crystallographically at the center of the Ru–Ru bond. Selected bond lengths (Å): Ru–Ru′ = 2.7430(4), Ru′–P(1) = 2.3710(7), Ru–P(2) = 2.3499(7), Ru–C(26) = 1.962(3), Ru–Cl = 2.3538(8), C(26)–O(1) = 1.188(3). Selected bond angles (°): Ru–Ru′–C(26) = 45.65(8), Ru′–Ru–C(26) = 46.32(8), Ru–C(26)–Ru′ = 88.03(12), Ru′–Ru–P(1′) = 95.01(2), Ru′–Ru–P(2) = 92.27(2), Ru′–Ru–Cl = 177.29(3), C(26)–Ru–C(26′) = 91.97(12).

surprise, all these values fall within the range for typical Ru–Ru single bond distances vide supra. By comparing the distances between the Ru atoms and the π-donor, X, in **3a**, **3c**, and **3e** with those in other similar compounds, Ru–X multiple, probably double, bonding interactions are believed to be present and lengthen the expected Ru–Ru triple bond into a single bond in **3a**, **3c** and **3e** (Scheme 2). The multiple Ru^{I}–X bonding interactions in these Ru_2^{2+} complexes are reflected by the relatively shorter Ru–Cl distance of 2.3538(8) Å in **3a**, in comparison with the terminal Ru–Cl distance of 2.409(4) Å in $[(\eta^5\text{-}C_5Me_5)Ru(\mu\text{-}NO)_2Cl]_2$ [9]; the relatively shorter values of 2.660(2) and 2.679(2) Å in **3c**, in comparison with the terminal Ru–I distance of 2.767(2) Å or with the bridging Ru–I distances of 2.756(2) and 2.825(2) Å in $[Ru_2(\mu\text{-}I)(\mu\text{-}CO)(CO)_2(\mu\text{-}DPPM)_2I]$ [8g]; and also by the relatively shorter Ru–S distance of 2.3282(6) Å in **3e**, in comparison with the bridging Ru–S distances of 2.4285(9) and 2.4358(11) Å in $[Ru_2(CO)_4(\mu\text{-}SPh)_2(PPh_3)_2]$ [8j]. Indeed, the direct evidence for the presence of a double Ru–Stol bond, and consequently a Ru–Ru single bond rather than a Ru–Ru triple bond in **3e**, is reflected in the angle, ∠Ru–S–C(tol), of 120.70(8)°, very close to the expected 120° for an sp^2 hybridized sulfur atom. Furthermore, a rather long S–C(tol) bond length of 1.785(2) Å in **3e**, relative to that of 1.52(2) Å in **6a**, described below (Fig. 7) was observed and this elongation can be attributed to the repulsion between the π-bonding electrons in the Ru–S double bond and those in the benzene ring (truly, the two π systems are not coplanar, as reflected in a torsion angle, ∠Ru(1)–S(1)–C(2)–C(3), of 114.2(2)°).

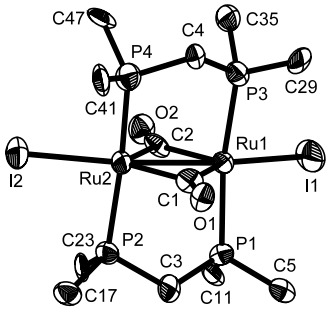

Fig. 3. ORTEP plot of **3c** with 50% thermal ellipsoids and the numbering scheme (only the *ipso* carbon atoms of each phenyl group have been retained for clarity). Selected bond lengths (Å): Ru(1)–Ru(2) = 2.738(2), Ru(1)–I(1) = 2.660(2), Ru(2)–I(2) = 2.679(2), Ru(1)–P(1) = 2.349(6), Ru(1)–P(3) = 2.346(6), Ru(2)–P(2) = 2.357(6), Ru(2)–P(4) = 2.349(6), Ru(1)–C(1) = 1.954(16), C(1)–O(1) = 1.18(2), Ru(2)–C(1) = 1.99(2), Ru(1)–C(2) = 1.95(2), C(2)–O(2) = 1.15(2), Ru(2)–C(2) = 2.013(16). Selected bond angles (°): Ru(2)–Ru(1)–P(1) = 93.90(15), Ru(2)–Ru(1)–P(3) = 92.81(15), Ru(1)–Ru(2)–P(2) = 93.19(15), Ru(1)–Ru(2)–P(4) = 92.83(15), Ru(2)–Ru(1)–I(1) = 165.15(8), Ru(1)–Ru(2)–I(2) = 165.15(9), I(1)–Ru(1)–C(1) = 148.3(6), C(1)–Ru(1)–C(2) = 93.7(7), C(2)–Ru(1)–I(1) = 117.9(5), I(2)–Ru(2)–C(1) = 149.4(5), C(1)–Ru(2)–C(2) = 90.9(7), C(2)–Ru(2)–I(2) = 119.7(6), Ru(1)–C(1)–Ru(2) = 88.0(7), Ru(1)–C(2)–Ru(2) = 87.3(7).

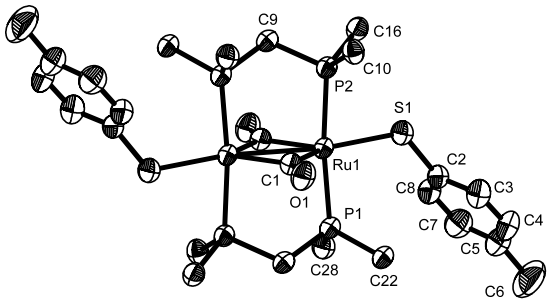

Fig. 4. ORTEP plot of **3e** with 50% thermal ellipsoids and the numbering scheme (only the *ipso* carbon atoms of each phenyl group attached to phosphorus atoms have been retained for clarity). An inversion center is imposed crystallographically at the center of the Ru–Ru bond. Selected bond lengths (Å): Ru(1)–Ru(1′) = 2.8091(3), Ru(1)–P(1) = 2.3546(6), Ru(1)–P(2) = 2.3779(6), Ru(1)–C(1) = 1.998(2), Ru(1)–C(1′) = 1.995(2), C(1)–O(1) = 1.189(2), Ru(1)–S(1) = 2.3282(6), S(1)–C(2) = 1.785(2). Selected bond angles (°): Ru(1′)–Ru(1)–P(1) = 93.707(16), Ru(1′)–Ru(1)–P(2) = 92.466(15), Ru(1′)–Ru(1)–S(1) = 172.972(19), C(1)–Ru(1)–C(1′) = 90.56(9), Ru(1)–C(1)–Ru(1′) = 89.44(9), Ru(1)–C(1)–O(1) = 135.55(16), Ru(1)–S(1)–C(2) = 120.70(8).

3.3. Reactions of *3a–c* and *3e–f*

Three typical reactions were carried out with three representative structures determined (Scheme 3). The reaction of **3a** with excess $Me_3NO{\cdot}2H_2O$ afforded two isomeric diamagnetic products **4a** and **4b**, with the formula $[Ru_2(CO)_2(\mu\text{-}DPPM)_2Cl_2(\mu\text{-}H)(\mu\text{-}OH)]$. The ratio **4a**–**4b** is 2.25, based on the ^{1}H-NMR evidence. These complexes appear to react with silica gel and only part of the converted products survived after 4 h separation. The yield obtained for **4a** is 16% and that for **4b** is 5%. Although the relevant formation mechanism is not known, a similar report concerning the formation of $[Os_3(CO)_{10}(NMe_3)(\mu_3\text{-}S)(\mu\text{-}OH)(\mu\text{-}H)]$

from the reaction of $[Os_3(CO)_{10}(\mu_3\text{-S})]$ and trimethylamine *N*-oxide dihydrate was described in the literature [10]. However, it is not clear at the moment about the source of the hydroxyl oxygen atom in the Os compound or our Ru complex, probably either from trimethylamine *N*-oxide or the hydrated water. However, good single crystals of the minor product **4b** were grown successfully, and the solid-state structure was determined. Importantly, this structure helps us to distinguish the two isomeric structures. The structure (Fig. 5) confirms the presence of two terminal carbonyls, a bridging hydride, and a bridging hydroxide rather than a bridging oxide or aqua based on solution ^{1}H-NMR and IR data. Clearly, the bridging hydride shows a virtual ^{1}H-NMR quintet at δ −26.36 for **4a** and δ −25.04 for **4b**. The bridging hydroxide displays only one weak IR O–H stretching band at 3627 cm^{-1} for **4a** and 3615 cm^{-1} for **4b**. The two terminal carbonyls are *trans* to the bridging hydroxide in **4b** (Fig. 5). Apparently the structure of the other isomer **4a** contains a different orientation with the stronger σ-donor, the μ-hydrido bridging ligand, *trans* to the carbonyls. This would explain why **4a** were formed in a larger quantity than **4b**. The Ru^{II}–Ru^{II} distance of 2.8620(7) Å in this compound, though much longer than the Ru^{I}–Ru^{I} distance of 2.7703(7) Å in **2** but comparable to that of 2.8091(3) Å in **3e**, may still indicate the presence of a single bond in spite of the maximum change in the metal–metal distances as large as 0.09 Å. The results achieved by

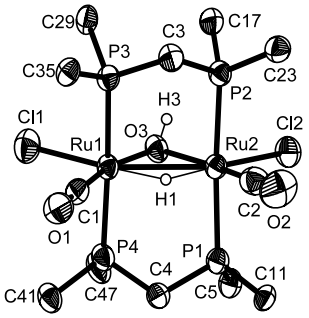

Fig. 5. ORTEP plot of **4b** with 50% thermal ellipsoids and the numbering scheme (only the *ipso* carbon atoms of each phenyl group have been retained for clarity). Selected bond lengths (Å): Ru(1)–Ru(2) = 2.8620(7), Ru(1)–Cl(1) = 2.438(2), Ru(2)–Cl(2) = 2.4169(17), Ru(1)–P(3) = 2.3829(18), Ru(1)–P(4) = 2.3719(19), Ru(2)–P(1) = 2.3751(19), Ru(2)–P(2) = 2.3646(19), Ru(1)–C(1) = 1.821(8), C(1)–O(1) = 1.152(9), C(1)–O(1) = 1.152(9), Ru(2)–C(2) = 1.816(10), C(2)–O(2) = 1.168(11), Ru(1)–O(3) = 2.161(4), Ru(2)–O(3) = 2.182(5), O(3)–H(3) = 0.804(10), Ru(1)–H(1) = 1.797(10), Ru(2)–H(1) = 1.748(10). Selected bond angles (°): Ru(2)–Ru(1)–P(3) = 91.28(4), Ru(2)–Ru(1)–P(4) = 91.68(5), Ru(1)–Ru(2)–P(1) = 91.90(5), Ru(1)–Ru(2)–P(2) = 91.73(5), P(1)–Ru(2)–P(2) = 175.97(7), P(3)–Ru(1)–P(4) = 176.02(6), Cl(1)–Ru(1)–O(3) = 97.60(14), O(3)–Ru(1)–Ru(2) = 49.09(13), C(1)–Ru(1)–Cl(1) = 93.1(2), Ru(1)–C(1)–O(1) = 178.4(7), Ru(1)–O(3)–Ru(2) = 82.44(17), Cl(2)–Ru(2)–O(3) = 97.79(13), O(3)–Ru(2)–Ru(1) = 48.47(11), C(2)–Ru(2)–Cl(1) = 177.7(8), Ru(1)–H(1)–Ru(2) = 35.6(1).

Alvarez and his co-workers [3f] showed that a variation as large as 0.255 Å in the Ru^{I}–Ru^{I} distances of $[Ru_2(bridge)_2(CO)_4L_n]$ complexes can be attributed to different pyramidal and torsional angles (the average pyramidal angle, α, in a range of 84.5–89.9° and the average torsional angle, τ, in a range of 0.0–28.5° are observed for the Ru–Ru distances, d(Ru–Ru), in a range of 2.630–2.885 Å [3f]. After a multilinear regression analysis, they obtained an equation that showed a fair correlation with a regression coefficient of 0.945: $d(\text{Ru–Ru}) = 2.296 + 3.148\cos\alpha + 0.353\cos 2\tau$. In other words, the Ru–Ru distance decreases more sensitively with increasing pyramidality than with increasing torsional angles). Their results prompted us to calculate the angles for our singly bonded diruthenium compounds and found (α, τ) = (92.7°, 1.7°) in **2**, (89.9°, 1.2°) in **3e**, and (89.1°, 8.5°) in **4b**. Clearly, their conclusion is applicable to our compounds, the smallest d(Ru–Ru) value of 2.7703(7) Å was observed for the largest α value of 92.7° in **2**, while the longest d(Ru–Ru) value of 2.8620(7) Å was observed for the shortest α value of 89.1° in **4b**.

Treatment of **3b** and **3c** with dimethyl acetylenedicarboxylate afforded $[Ru_2(\mu\text{-CO})(\mu\text{-DPPM})_2(\mu\text{-MeO}_2CCCCO_2Me)X_2]$ (X = Br, **5a**; I, **5b**) as the only product. The structure of **5a** was also determined using X-ray diffraction methods (Fig. 6). The alkyne molecule is bound to the metals as a *cis*-dimetalated olefin (i.e. in an μ-II mode [11]); therefore, all angles about C(2) and C(3) are close to 120° as expected for sp^2-hybridization of these atoms. The distortion from idealized sp^2-hybridization results from the strain imposed by the Ru–Ru bond vide infra which compresses the Ru(1)–C(2)–C(3) and Ru(2)–C(3)–C(2) angles to 114.6(2) and 110.1(6)°, respectively. Similar distortions were observed in other metal–metal bonded species with analogously bound acetylene ligands [11a]. When no metal–metal bond is present, the acetylene ligands are found to approach more closely the olefin geometry [11b,11c,11d]. In spite of the strain in the acetylene molecule, the ruthenium atoms and the carbon atom framework of the acetylene ligand are quite planar with the torsional angle, ∠Ru(1)–C(2)–C(3)–Ru(2) = 0.8(8)°. On the basis of the observed strain in the molecule, one might expect that the resulting metal–acetylene orbital overlap would be less than in unstrained cases, resulting in less acetylene activation. However, the other structural parameters in the ligand do not confirm this expectation. The ruthenium–acetylene bonds (d(Ru(1)–C(2)) = 2.039(8) and d(Ru(2)–C(3)) = 2.034(8) Å) are among the shortest observed for diruthenium acetylene-bridged complexes, and the acetylene C–C bond (i.e. C(2)–C(3), 1.336(11) Å) is consistently among the longest observed [12]. The distances between Ru and acetate oxygen atoms are d(Ru(1)–O(3)) = 2.624(6) Å and d(Ru(2)–O(5)) =

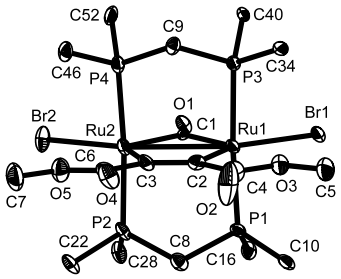

Fig. 6. ORTEP plot of **5a** with 50% thermal ellipsoids and the numbering scheme (only the *ipso* carbon atoms of each phenyl group have been retained for clarity). Selected bond lengths (Å): Ru(1)–Ru(2) = 2.8717(9), Ru(1)–Br(1) = 2.5350(10), Ru(2)–Br(2) = 2.5246(10), Ru(1)–P(1) = 2.363(2), Ru(1)–P(3) = 2.374(2), Ru(2)–P(2) = 2.366(2), Ru(2)–P(4) = 2.374(2), Ru(1)–C(1) = 1.972(7), Ru(2)–C(1) = 1.996(7), C(1)–O(1) = 1.161(9), Ru(1)–C(2) = 2.039(8), Ru(2)–C(3) = 2.034(8), C(2)–C(3) = 1.336(11), C(2)–C(4) = 1.485(12), C(3)–C(6) = 1.466(11), C(4)–O(2) = 1.192(12), C(6)–O(4) = 1.197(11), C(4)–O(3) = 1.334(11), C(6)–O(5) = 1.364(10), O(3)–C(5) = 1.462(11), O(5)–C(7) = 1.449(12). Selected bond angles (°): Ru(2)–Ru(1)–P(1) = 91.87(5), Ru(2)–Ru(1)–P(3) = 92.24(5), Ru(1)–Ru(2)–P(2) = 91.99(5), Ru(1)–Ru(2)–P(4) = 92.07(5), Ru(2)–Ru(1)–Br(1) = 147.75(4), Ru(1)–Ru(2)–Br(2) = 152.51(4), Br(1)–Ru(1)–C(1) = 103.8(2), C(1)–Ru(1)–C(2) = 110.8(3), Ru(1)–C(2)–C(3) = 114.2(6), C(2)–C(3)–Ru(2) = 110.1(6), C(3)–Ru(2)–C(1) = 112.2(3), Ru(2)–C(1)–O(1) = 129.8(6), Ru(2)–C(1)–Ru(1) = 92.7(3), Ru(1)–C(1)–O(1) = 137.5(6), Br(1)–Ru(1)–C(2) = 145.4(2), Br(2)–Ru(2)–C(1) = 109.2(2), Br(2)–Ru(2)–C(3) = 138.6(2).

2.829(6) Å, far beyond the expected single-bond distance of 2.12 Å, calculated based on the reported distance of 2.16 Å found in $[Re_2(CO)_9(\mu\text{-}HCCCO_2Me)]$ [13] and the smaller covalent radius for Ru [14]. The Ru–Ru distance is 2.8717(9) Å, similar to that of 2.8620(7) Å in **4b**. Apparently it is a single bond distance, although a 'triple' Ru–Ru bond is expected again in **5a**, based on the 18-electron rule with both Br atoms as the two-electron donors. The shorter terminal Ru^{II}–Br distances with $d(Ru(1)–Br(1)) = 2.535(1)$ Å and $d(Ru(2)–Br(2)) = 2.525(1)$ Å in **5a**, compared with that of 2.543(4) Å in $[Ru_2Br_2(\mu\text{-}Br)_2(CO)_6]$ [15] may indicate the presence of multiple (probably double) Ru–Br bonding interactions, which then lengthen the 'triple' Ru–Ru distance to the single-bond value. Further, the observed Ru–Ru distance of 2.8717(9) Å can be considered as 'expected', by considering the pyramidal and torsional effects on the metal–metal single bond length vide supra. This value co-exists with the averaged pyramidal angle, α, of 89.1° and with the averaged torsion angle, τ, of 1.0° in **5a**. Since the pyramidal angle is identical to that in **4b**, the significantly longer Ru–Ru bond length of 2.8717(9) Å in **5a**, relative to that of 2.8620(7) Å in **4b**, is probably caused by the smaller torsion angle of 1.0° in **5a**, compared with that of 8.5° in **4b**.

Iodination of the singly Ru–Ru and doubly Ru–S bonded complexes, **3e** and **3f** is a complicated reaction, from which a diamagnetic compound $[Ru_2(CO)_2(\mu\text{-}DPPM)_2I_2(\mu\text{-}I)(\mu\text{-}SR)]$ (R = tol, **6a**; ^{i}Pr, **6b**) was isolated. The solid-state structure of **6a** (Fig. 7) was determined using X-ray diffraction methods to reveal the loss of one doubly bonded RS group, isomerization of the remaining RS group from the terminal to the bridging position, coordination of three I atoms in one bridging and two terminal positions, and the cleavage of the Ru–Ru single bond, as reflected in the long Ru(1)–Ru(2) separation of 3.687(2) Å. The singly bonded Ru^{II}–I distances in either terminal ($d(Ru(1)–I(1)) = 2.746(2)$ and $d(Ru(2)–I(3)) = 2.765(2)$ Å) or bridging positions ($d(Ru(1)–I(2)) = 2.759(2)$ Å and $d(Ru(2)–I(2)) = 2.752(2)$ Å) are longer as expected in **6a** (Fig. 7) than the partially doubly bonded Ru^{I}–I distances ($d(Ru(1)–I(1)) = 2.660(2)$ and $d(Ru(2)–I(2)) = 2.679(2)$ Å) in **3c** (Fig. 3). The bridging SR^- group is not coplanar with two Ru atoms, as reflected in the torsional angle, ∠ Ru(1)–Ru(2)–S(1)–C(3), of 136.7(9)°. The S atom is apparently in sp^3-hybridization and the SR^- group acts as a four-electron donor, donating two electrons to each Ru atom. The similarity in the Ru–I distances (i.e. Ru–I(terminal) and Ru–I(bridging)) indicates that the bridging I^- atom may also act as a four-electron donor, donating two electrons to each Ru atom in the complex. The electron count for each Ru atom thus reaches 18, explaining the observed diamagnetic property for **6a** and **6b**.

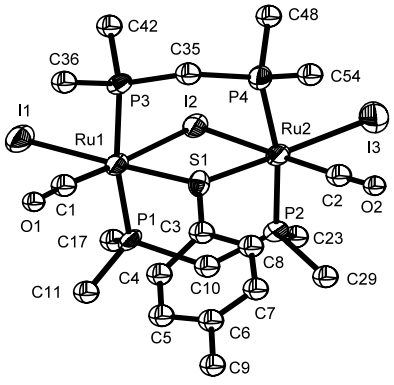

Fig. 7. ORTEP plot of **6a** with 50% thermal ellipsoids and the numbering scheme (only the *ipso* carbon atoms of each phenyl group have been retained for clarity). Selected bond lengths (Å): Ru(1)–I(1) = 2.746(2), Ru(1)–I(2) = 2.759(2), Ru(2)–I(2) = 2.752(2), Ru(2)–I(3) = 2.765(2), Ru(1)–P(1) = 2.398(5), Ru(1)–P(3) = 2.402(5), Ru(2)–P(2) = 2.374(5), Ru(2)–P(4) = 2.418(5), Ru(1)–C(1) = 1.84(2), C(1)–O(1) = 1.10(2), Ru(2)–C(2) = 1.93(2), C(2)–O(2) = 1.04(2), Ru(1)–S(1) = 2.407(4), Ru(2)–S(1) = 2.396(5), S(1)–C(3) = 1.52(2). Selected bond angles (°): P(1)–Ru(1)–P(3) = 170.1(2), P(2)–Ru(2)–P(4) = 169.3(2), I(1)–Ru(1)–I(2) = 94.05(6), I(2)–Ru(1)–S(1) = 87.66(12), S(1)–Ru(1)–C(1) = 92.4(6), C(1)–Ru(1)–I(1) = 85.7(5), Ru(1)–I(2)–Ru(2) = 83.99(6), Ru(1)–S(1)–Ru(2) = 100.3(2), Ru(1)–S(1)–C(3) = 121.0(8), Ru(2)–S(1)–C(3) = 121.9(7), I(2)–Ru(2)–I(3) = 96.21(7), I(2)–Ru(2)–S(1) = 88.04(12), S(1)–Ru(2)–C(2) = 94.7(6), C(2)–Ru(2)–I(3) = 81.2(6), Ru(1)–C(1)–O(1) = 174(2), Ru(2)–C(2)–O(2) = 174(2).

4. Conclusions

Our investigation into the acetate-removal of $[Ru_2(CO)_4(\mu\text{-DPPM})_2(\mu\text{-OAc})]^+$ **[1]**$^+$ with $Et_3O^+BF_4^-$ in MeCN resulted in the formation of versatile products $[Ru_2(\mu\text{-CO})_2(\mu\text{-DPPM})_2(MeCN)_4]^{2+}$ **[2]**$^{2+}$ (Scheme 1). Upon addition of an excess amount of a uninegative anion X^- to a solution of **2** in MeCN, a series of neutral, coordinatively unsaturated adducts $[Ru_2(\mu\text{-CO})_2(\mu\text{-DPPM})_2X_2]$ ($X^- = Cl^-$, **3a**; Br^-, **3b**; I^-, **3c**; SH^-, **3d**; $Stol^-$, **3e**; S^iPr^-, **3f**) were readily formed (Scheme 2). The reaction of **3a** with $Me_3NO{\cdot}2H_2O$ afforded two isomeric products of $[Ru_2(CO)_2(\mu\text{-DPPM})_2Cl_2(\mu\text{-H})(\mu\text{-OH})]$ at a ratio of **4a**–**4b** = 2.25. Treatment of **3b** and **3c** with dimethyl acetylenedicarboxylate produced $[Ru_2(\mu\text{-CO})(\mu\text{-DPPM})_2X_2(\mu\text{-}MeO_2CCCCO_2Me)]$ (X = Br, **5a**; I, **5b**), whereas treatment of **3e** and **3f** with I_2 yielded $[Ru_2(CO)_2(\mu\text{-DPPM})_2I_2(\mu\text{-I})(\mu\text{-SR})]$ (R = tol, **6a**; ^{i}Pr, **6b**) (Scheme 3). Structures **2**, **3a**, **3c**, **3e**, **4b**, **5a** and **6a** in Figs. 1–7, respectively, were described. The observed Ru–Ru distances are compared and explained in terms of both electronic and steric effects by considering the multiple metal–ligand (M–X) bonding interactions and Alvarez's structural parameters including M–M–X pyramidal angles and the X–M–M–X torsional angles.

5. Supplementary material

Crystallographic data for the structural analysis has been deposited with the Cambridge Crystallographic Data Centre, CCDC Nos. 187200–187206 for compounds **2**, **3a**, **3c**, **3e**, **4b**, **5a**, and **6a** respectively. Copies of this information may be obtained free of charge from: The Director, CCDC, 12 Union Road, Cambridge, CB2 1EZ, UK (Fax: +44-1223-336033; e-mail: deposit@ccdc.cam.ac.uk or www: http://www.ccdc.cam.ac.uk).

Acknowledgements

Financial support for this work by the National Science Council of Republic of China (Contracts NSC89-2113-M006-019 and NSC90-2113-M-006-021) is gratefully acknowledged.

References

[1] K.-B. Shiu, S.-S. Yang, S.-I. Chen, J.-Y. Chen, H.-J. Wang, S.-L. Wang, F.-L. Liao, S.-M. Peng, Y.-H. Liu, Organometallics 18 (1999) 4244.
[2] W.A. Nugent, J.M. Mayer, Metal–Ligand Multiple Bonds, Wiley, New York, 1988.
[3] (a) J. Losada, S. Alvarez, J.J. Novoa, F. Mota, J. Am. Chem. Soc. 112 (1990) 8998;
(b) F. Mota, J.J. Novoa, J. Losda, S. Alvarez, R. Hoffman, J. Sivestre, J. Am. Chem. Soc. 115 (1993) 6216;
(c) G. Aullon, S. Alvarez, Inorg. Chem. 32 (1993) 3712;
(d) J.J. Novoa, G. Aullon, P. Alemany, S. Alvarez, J. Am. Chem. Soc. 117 (1995) 7169;
(e) G. Aullon, P. Alemany, S. Alvarez, Inorg. Chem. 35 (1996) 5061;
(f) G. Aullon, S. Alvarez, J. Chem. Soc. Dalton Trans. (1997) 2681;
(g) X.-Y. Liu, S. Alvarez, Inorg. Chem. 36 (1997) 1055;
(h) G. Aullon, S. Alvarez, Chem. Eur. J. 3 (1997) 655.
[4] S.J. Sherlock, M. Cowie, E. Singleton, M.M. de, V. Steyn, Organometallics 7 (1988) 1663.
[5] E.J. Gabe, Y. Le Page, J.-P. Charland, F.L. Lee, P.S. White, J. Appl. Crystallogr. 22 (1989) 384.
[6] G.M. Sheldrick, SHELXTL-PLUS Crystallographic System, Release 4.21, Siemens Analytical X-ray Instruments, Madison, WI, 1991.
[7] K.-B. Shiu, C.-H. Li, T.-J. Chan, S.-M. Peng, M.-C. Cheng, S.-L. Wang, F.-L. Liao, M.-Y. Chiang, Organometallics 14 (1995) 524.
[8] (a) S.J. Sherlock, M. Cowie, E. Singleton, M.M. de Steyn, J. Organomet. Chem. 361 (1989) 353;
(b) P.L. Andren, J.A. Cabeza, V. Riera, F. Jennin, J. Organomet. Chem. 372 (1989) C15;
(c) S. Garcia-Granda, R. Obeso-Rosete, J.M.R. Gonzalez, A. Anillo, Acta Crystallogr. Sect. C 46 (1990) 2043;
(d) G. Rheinwald, H. Stoeckli-Evans, G. Suss-Fink, J. Organomet. Chem. 441 (1992) 295;
(e) K.-B. Shiu, S.-M. Peng, M.-C. Cheng, J. Organomet. Chem. 452 (1993) 143;
(f) W.G. Klemperer, Z. Bianxia, Inorg. Chem. 32 (1993) 5821;
(g) K.-B. Shiu, W.-N. Guo, T.-J. Chan, J.-C. Wang, L.-S. Liou, S.-M. Peng, M.-C. Cheng, Organometallics 14 (1995) 1732;
(h) K.-B. Shiu, L.-T. Yang, S.-W. Jean, C.-H. Li, R.-R. Wu, J.-C. Wang, L.-S. Liou, M.-Y. Chiang, Inorg. Chem. 35 (1996) 7845;
(i) K.-B. Shiu, S.-W. Jean, H.-J. Wang, S.-L. Wang, F.-L. Liao, J.-C. Wang, L.-S. Liou, Organometallics 16 (1997) 114;
(j) K.-B. Shiu, S.-L. Wang, F.-L. Liao, M.-Y. Chiang, S.-M. Peng, G.-H. Lee, J.-C. Wang, L.-S. Liou, Organometallics 17 (1998) 1790.
[9] J.L. Hubbard, A. Morneau, R.M. Burns, C.R. Zoch, J. Am. Chem. Soc. 113 (1991) 9176.
[10] R.D. Adams, J.E. Babin, H.S. Kim, Inorg. Chem. 25 (1986) 1122.
[11] (a) C.-L. Lee, C.T. Hunt, A.L. Balch, Inorg. Chem. 20 (1981) 2489;
(b) M. Cowie, R.S. Dickson, Inorg. Chem. 20 (1981) 2682;
(c) B.L. Shaw, S.J. Higgins, J. Chem. Soc. Dalton Trans. (1988) 457;
(d) J.T. Mague, Polyhedron 11 (1992) 677.
[12] (a) J.S. Field, R.J. Haines, J. Sundermeyer, S.F. Woollam, J. Chem. Soc. Dalton Trans. (1993) 3749;
(b) J. Kuncheria, H.A. Mirza, R.J. Puddephatt, J. Organomet. Chem. 593–594 (2000) 77.
[13] R.D. Adams, L. Chen, W. Wu, Organometallics 12 (1993) 1257.
[14] J. Emsley, The Elements, Oxford University Press, New York, 1989.
[15] S. Merlino, G. Montagnoli, Acta Crystallogr. Sect. B 24 (1968) 424.